from spectral data. Excitation through a resonance level, however, should be energy-dependent (*19*). Electronic structure calculations (*17*, *23*) and experiments (*24*, *25*) point to the onset of a σ*(Si–H) empty level in the relevant energy range, roughly 2 to 3 eV above the Fermi level. The inelastic fractions that quantitatively account for the experimental observations, as indicated in Fig. 4, are in rough agreement with expectations based on the profile of this resonance. We thus conclude that the H atom desorption mechanism in the energy range from about 2 to 5 eV can be described as resonantly enhanced multiple-vibrational excitation.

The use of tunneling electrons in place of field-emitted electrons to desorb H atoms makes possible STM lithography with atomic resolution. An example involving a pattern of parallel lines at 30 Å pitch written with $V_s = +3$ V is shown in Fig. 5. The lines are, for the most part, composed of single Si atom dangling bonds or Si dimer dangling bonds corresponding to a resolution of <10 Å. Figure 5 shows that the vibrational mechanism can lead to single H atom desorption. However, because of their close proximity and the high current densities utilized, often both H atoms on a single dimer are desorbed (see arrows).

Dangling bond patterns such as that in Fig. 5 can be converted to chemical modification patterns if the selectively depassivated surface is exposed to reactive gases (*7*). Vibrational excitation of adsorbates with atomic resolution opens up many other possibilities for selective activation, either directly or through subsequent energy transfer to other degrees of freedom, of processes such as adsorbate dissociation, bimolecular reaction, and diffusion (*26*).

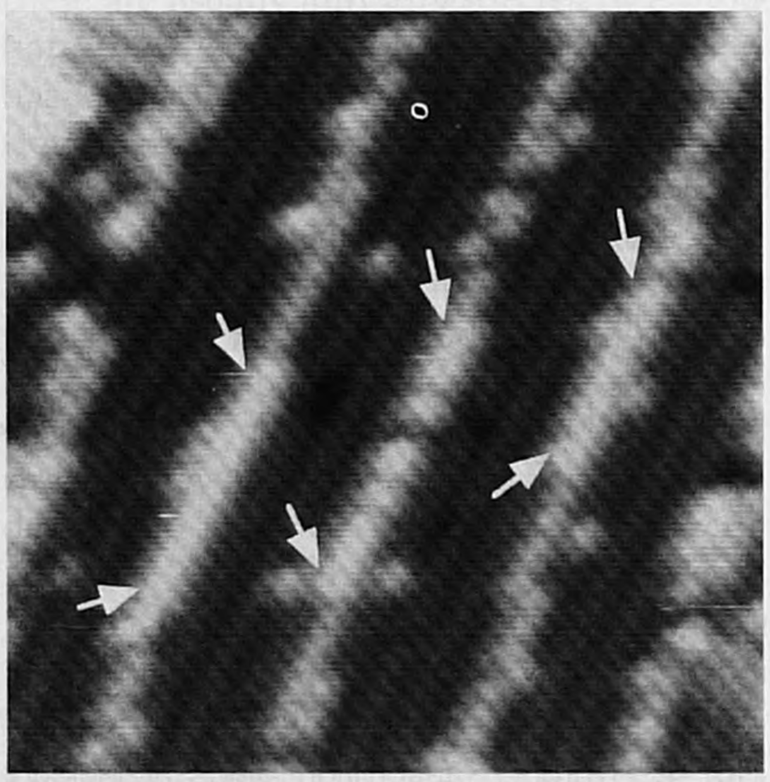

Fig. 5. An STM image (150 Å by 150 Å, $V_s = -1.4$ V, $I = 0.1$ nA) showing a pattern of 30 Å pitch lines of dangling bonds written with $V_s = +3$ V, $I = 4.5$ nA, and $Q = 6 \times 10^{-4}$ C/cm. The arrows point to sites at which both H atoms of an Si dimer have been desorbed.

REFERENCES AND NOTES

1. Ph. Avouris, Ed., *Atomic and Nanometer Scale Modification of Materials: Fundamentals and Applications* (Kluwer, Dordrecht, Netherlands, 1993).
2. C. A. Quate, in *Highlights in Condensed Matter Physics*, L. Esaki, Ed. (Plenum, New York, 1991), pp. 573–630.
3. J. A. Stroscio and D. M. Eigler, *Science* **254**, 1319 (1991).
4. R. D. Ramsier and J. T. Yates Jr., *Surf. Sci. Rep.* **12**, 243 (1991).
5. Ph. Avouris and R. E. Walkup, *Annu. Rev. Phys. Chem.* **40**, 173 (1989).
6. E. S. Snow and P. M. Cambell, *Appl. Phys. Lett.* **64**, 1932 (1994).
7. J. W. Lyding, T.-C. Shen, J. S. Hubacek, J. R. Tucker, G. C. Abeln, *ibid.*, p. 2010.
8. R. S. Becker, G. S. Higashi, Y. J. Chabal, A. J. Becker, *Phys. Rev. Lett.* **65**, 1917 (1990).
9. R. E. Walkup, D. M. Newns, Ph. Avouris, in (*1*), pp. 97–109.
10. ———, *Phys. Rev. B* **48**, 1858 (1993).
11. B. N. J. Persson, *ibid.* **44**, 3277 (1991).
12. P. Guyot-Sionnest, P. Dumas, Y. J. Chabal, G. S. Higashi, *Phys. Rev. Lett.* **64**, 2156 (1990).
13. P. Guyot-Sionnest, P. H. Lin, E. M. Miller, *J. Chem. Phys.*, **102**, 4269 (1995).
14. J. J. Boland, *Surf. Sci.* **261**, 17 (1992).
15. D. T. Jiang, G. W. Anderson, K. Griffiths, T. K. Sham, P. R. Norton, *Phys. Rev. B* **48**, 4952 (1993).
16. S. Maruno, H. Iwasaki, K. Horioka, S.-T. Li, S. Nakamura, *ibid.* **27**, 4110 (1983).
17. S. Ciraci, R. Butz, E. M. Oelling, H. Wagner, *ibid.* **30**, 711 (1984).
18. K. P. Huber and G. Herzberg, *Molecular Spectra and Molecular Structure* (Van Nostrand Reinhold, New York, 1979).
19. B. N. J. Persson, *Phys. Scr.* **38**, 282 (1988).
20. N. G. van Kempen, *Stochastic Processes in Physics and Chemistry* (North-Holland, Amsterdam, 1981).
21. Y. J. Chabal and K. Raghavachari, *Phys. Rev. Lett.* **53**, 282 (1984).
22. B. N. J. Persson and A. Baratoff, *ibid.* **59**, 339 (1987).
23. M. Schlüter and M. L. Cohen, *Phys. Rev. B* **17**, 716 (1978).
24. L. S. O. Johansson, R. I. G. Uhrberg, G. V. Hansson, *ibid.* **38**, 13490 (1988).
25. J. Wintterlin and Ph. Avouris, *J. Chem. Phys.* **100**, 687 (1994).
26. Ph. Avouris, *Acc. Chem. Res.* **28**, 95 (1995).

27. This work is supported by an Office of Naval Research University Research Initiative under grant N00014-92-J-1519. We acknowledge valuable discussions with P. von Allmen (T.-C.S.), B. N. J. Persson (Ph.A.), and P. Guyot-Sionnest (Ph.A.). We thank T. M. Jackman, who provided valuable help with graphics.

25 January 1995; accepted 28 March 1995

Polystyrene-Dendrimer Amphiphilic Block Copolymers with a Generation-Dependent Aggregation

J. C. M. van Hest, D. A. P. Delnoye, M. W. P. L. Baars, M. H. P. van Genderen, E. W. Meijer*

A class of amphiphilic macromolecules has been synthesized by combining well-defined polystyrene (PS) with poly(propylene imine) dendrimers. Five different generations, from PS-*dendr*-NH_2 up to PS-*dendr*-$(NH_2)_{32}$, were prepared in yields of 70 to 90 percent. Dynamic light scattering, conductivity measurements, and transmission electron microscopy show that in aqueous phases, PS-*dendr*-$(NH_2)_{32}$ forms spherical micelles, PS-*dendr*-$(NH_2)_{16}$ forms micellar rods, and PS-*dendr*-$(NH_2)_8$ forms vesicular structures. The lower generations of this class of macromolecules show inverted micellar behavior. The observed effect of amphiphile geometry on aggregation behavior is in qualitative agreement with the theory of Israelachvili *et al*. The amphiphiles presented here are similar in shape but different in size as compared with traditional surfactants, whereas they are similar in size but different in shape as compared with traditional block copolymers.

The synthesis and characterization of new amphiphilic structures is one of the most daring and promising approaches toward a better understanding of the structure-property relation of amphiphiles (*1*). Historically, the field has been subdivided into traditional surfactants and amphiphilic block copolymers. Both classes have been subjected to extensive studies (*2*–*4*), but a detailed comparison between surfactants and block copolymers that would make it possible to understand the effect of increasing size and shape on aggregation has not been possible, because of distinct differences in the polar segments. The low–molecular weight surfactants have a compact polar head group, whereas the block copolymers known thus far have linear, extendable polar chains.

Recently, dendrimers, which are well-defined and highly branched macromolecules that emanate from a central core, have begun to receive scientific attention (*5*). These spherical structures have been proposed as precise nanoscopic building blocks (*6*). New architectures have been synthesized (*7*), including unimolecular micelles and structures containing dendrimers and linear macromolecules (*8*). Chapman *et al*. (*9*) presented hydra-amphiphiles that

Laboratory of Organic Chemistry, Eindhoven University of Technology, Post Office Box 513, 5600 MB Eindhoven, Netherlands.

*To whom correspondence should be addressed.

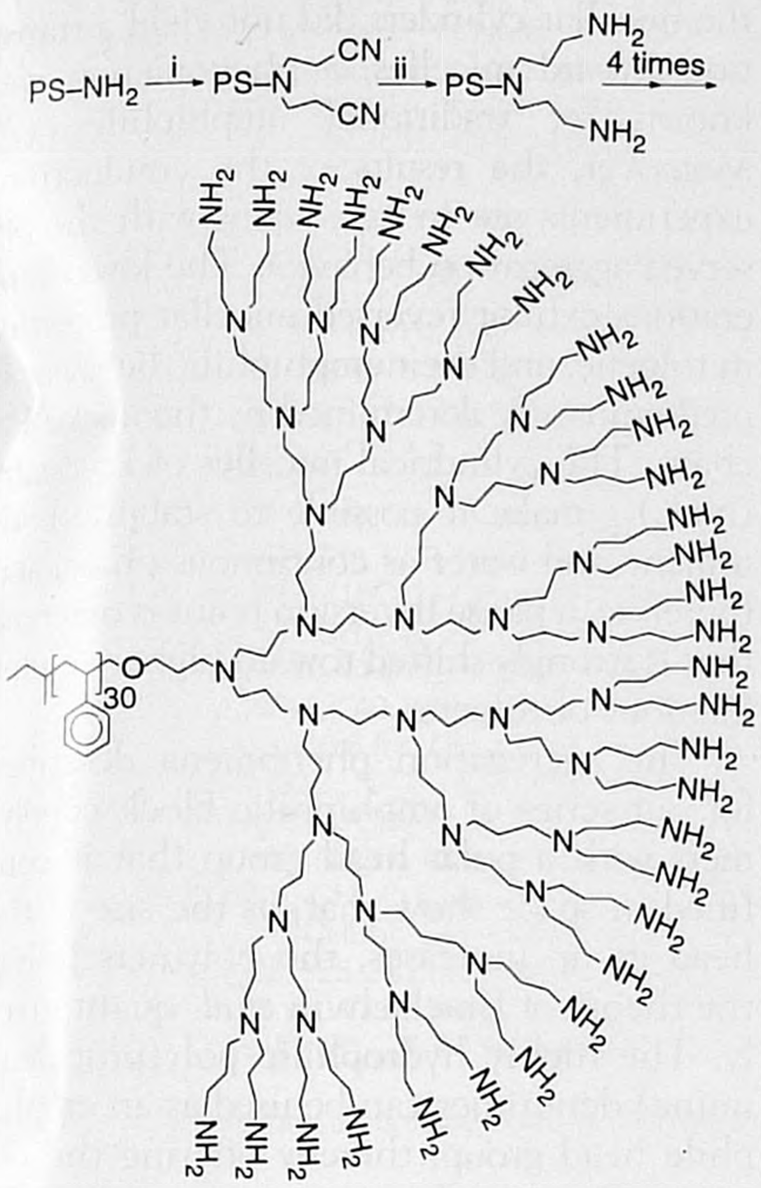

Scheme 1. Synthetic route toward PS-*dendr*-$(NH_2)_{32}$: (i) cyanoethylation with acrylonitrile in water-toluene, catalyzed by acetic acid; (ii) hydrogenation at 80-bar H_2 pressure, with Raney cobalt as catalyst.

consist of a dendrimer as the apolar part and a poly(ethylene oxide) chain as the polar part. The amphiphilic polymers described by Zhong and Eisenberg (*10*) can be regarded as the first approach toward PS-dendrimer structures with variable polar headgroup size. Poly(propylene imine) dendrimers are very hydrophilic (*11*). These sphere-like structures with diameters of 1 to 4 nm are synthesized in a reaction sequence consisting of two steps: a double cyanoethylation of primary amines with acrylonitrile, followed by Raney cobalt hydrogenation of the nitriles to the primary amines. The combination of hydrophilicity and a highly branched structure makes these dendrimers interesting building blocks for use as the polar part in amphiphilic block copolymers. We report on the synthesis and characterization of a well-defined class of hybrid PS-dendrimer block copolymers for which the head-group size is varied. The structures presented here can be seen as a type of amphiphiles intermediate between the traditional organic surfactants and amphiphilic block copolymers, with the size of the latter and the shape of the former.

Our first target molecule was a block copolymer with a PS chain of low molecular weight and a poly(propylene imine) dendrimer of the fifth generation, in this case with 32 primary amine end groups. The synthesis we used is depicted in Scheme 1. For the PS part we applied the anionic polymerization technique, which gives full control over molecular weight and allows the introduction of a reactive end-group functionality. The starting point of the divergent dendrimer synthesis, the primary amine end group of PS, was successfully introduced through an indirect method starting from OH-functionalized PS ($M_n = 3 \times 10^3$ g/mol, $M_w/M_n = 1.05$, where M_n is the number average molecular weight and M_w is the weight average molecular weight). The use of amine-functionalized PS as the core molecule for the poly(propylene imine) dendrimer synthesis, in combination with the amphiphilic character of the intermediates, required the reoptimization of most of the reaction steps in the dendrimer synthesis.

The choice of solvent combination for the cyanoethylation was of considerable importance. The reaction proceeded best when a heterogeneous system of toluene and water was used, with acetic acid as catalyst. Purifications could be performed by precipitation techniques and by column chromatography up to PS-*dendr*-CN_{16}. All of the nitrile intermediates could be synthesized quantitatively with yields after work-up between 70 and 90%. We performed hydrogenations in an NH_3-saturated toluene-methanol mixture at an H_2 pressure of 80 bars, using Raney cobalt as catalyst. To obtain yields after work-up of more than 90%, we found it necessary to work at a scale of at least 5 to 10 g; in that case, difficulties in the characterization were prevented as well (*12*). All of the spectroscopic data are in full agreement with the structures presented. Proton nuclear magnetic resonance (^1H NMR) measurements could be performed in $CDCl_3$. Only with PS-*dendr*-$(NH_2)_{32}$ were significant solubility problems encountered. With ^{13}C NMR, it was possible to distinguish between the different dendrimeric layers of the molecules. Electrospray mass spectroscopy was used to establish an overall purity of more than 95% for PS-*dendr*-$(NH_2)_8$. Energy-minimized structures, determined from CHARMm molecular mechanics calculations of PS-*dendr*-$(NH_2)_{16}$ and PS-*dendr*-$(NH_2)_{32}$, are presented in Fig. 1. Obviously, only one of the possible conformations is visualized (*13*).

The developing amphiphilic character of the intermediates was clearly noticed during the cyanoethylation experiments. In the heterogeneous reaction system, the cyanoethylation takes place at the toluene-water interface. At higher generations, the increasing polarity of the head groups made it necessary to adjust the toluene-water ratio from 2:1 to 1:1 by volume. The role of NH_3 during hydrogenation is crucial; it displaces primary amines from the catalyst surface, which results in an enhanced reaction rate. Furthermore, it prevents the intramolecular side reaction of an amine with an imine, leading to the formation of

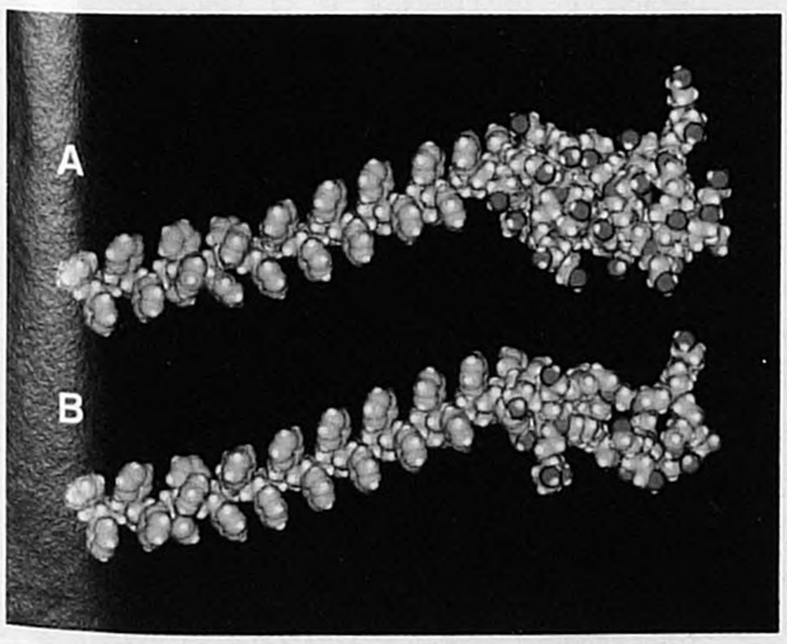

Fig. 1. Images of (**A**) PS-*dendr*-$(NH_2)_{32}$ and (**B**) PS-*dendr*-$(NH_2)_{16}$. We obtained the three-dimensional images by modeling with Quanta 3.3 and subsequently performing minimalizations with CHARMm 22, using the steepest descent followed by the conjugate gradient methods. Green atoms: carbon; white atoms: hydrogen; blue: nitrogen; and red: oxygen.

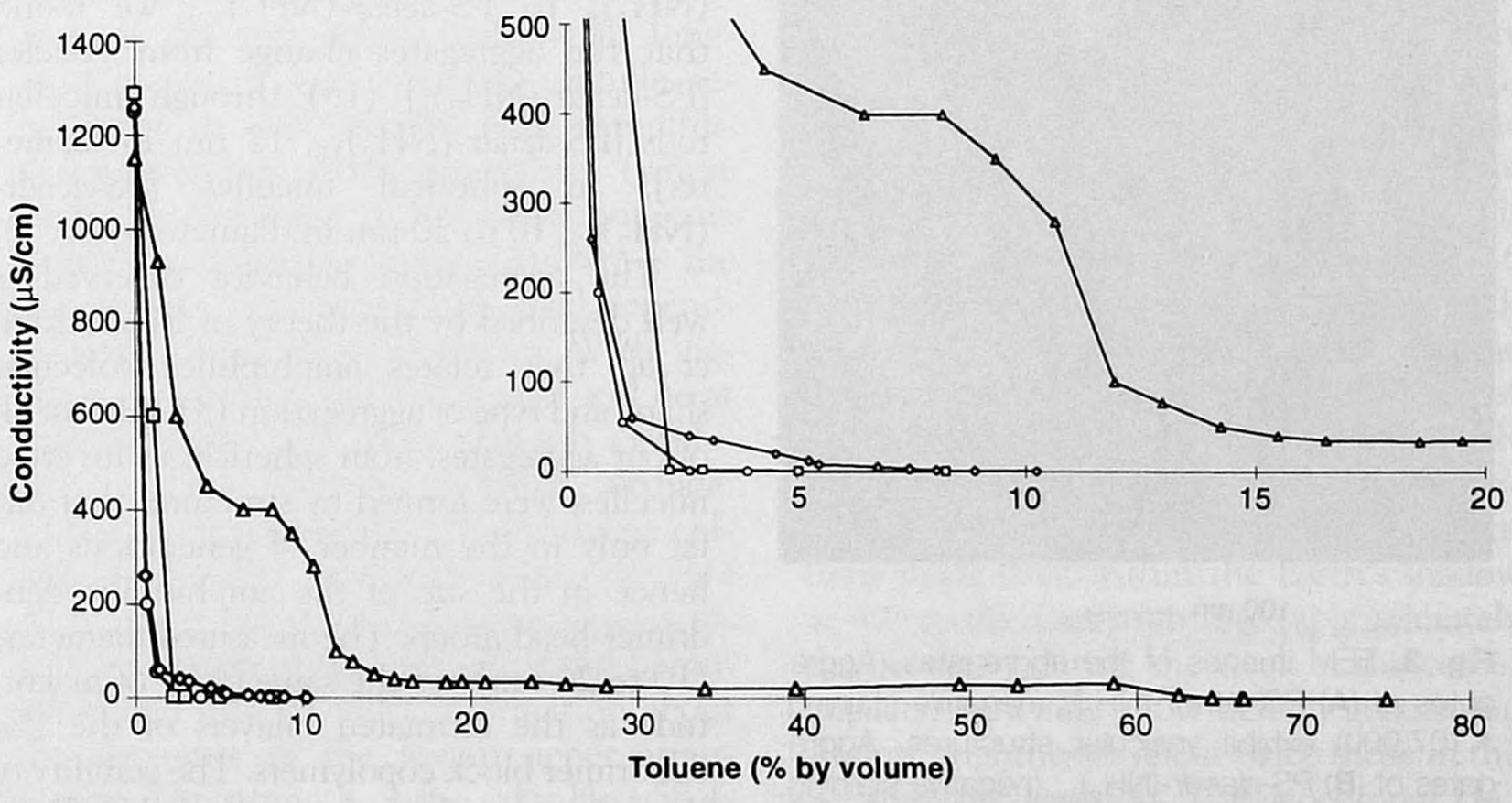

Fig. 2. Conductivity measurements of toluene-water systems in the presence of PS-*dendr*-$(NH_2)_n$, (○: $n = 2$, □: $n = 4$, ◇: $n = 8$ and △: $n = 16$). The inset is an enlargement of the area from 0 to 20% toluene by volume.

secondary amines. Without NH_3, it was impossible to hydrogenate even PS-*dendr*-$(CN)_4$ quantitatively.

We studied the amphiphilic behavior of PS-*dendr*-$(NH_2)_n$ by making conductivity measurements and by using dynamic light scattering (DLS) and transmission electron microscopy (TEM). Conductivity measurements were performed to study the amphiphilic properties in toluene-water mixtures. A 3×10^{-4} M amphiphile solution in toluene was added dropwise to an aqueous 0.01 M KCl solution, in which 3×10^{-4} mol of amphiphile was dispersed per liter. By measuring the conductivity of the system as a function of the toluene/water ratio, we could identify the point of phase inversion from water to toluene as the continuous phase (Fig. 2). All lower generation amphiphiles showed a strong tendency to stabilize toluene as the continuous phase. The PS-*dendr*-$(NH_2)_2$ system even showed a remarkable phase inversion at 2% by volume of toluene. We found that PS-*dendr*-$(NH_2)_{16}$ has the highest inversion point, well beyond 50% toluene by volume; the inversion point of PS-*dendr*-$(NH_2)_{32}$ could not be measured in the same way, because this block copolymer is insoluble in toluene.

The differences in amphiphilic behavior suggested differences in the type of aggregation of these amphiphiles, and DLS and TEM were used to investigate these aggregates. The DLS measurements were performed on aqueous aggregates of PS-*dendr*-$(NH_2)_n$ (where n = 8 to 32) and on PS-*dendr*-$(NH_2)_4$ in toluene. The latter showed inverted micellar behavior with a radius of 3.4 nm. For PS-*dendr*-$(NH_2)_{16}$, complicated structures were observed that could be identified as large threadlike structures with a hydrodynamic radius of 120 nm. DLS measurements on the other generations in water were hampered by clustering between the aggregates. Therefore, we used TEM to obtain the ultimate evidence about the aggregation behavior. The aqueous aggregates of PS-*dendr*-$(NH_2)_n$ (n = 8, 16, or 32) (3×10^{-4} mol/liter) (*14*) were studied with three different techniques: negative staining with uranyl acetate, Pt shadowing, and freeze fracture. All three techniques showed the same results. On examining PS-*dendr*-$(NH_2)_8$ to PS-*dendr*-$(NH_2)_{32}$, we found that the aggregates change from vesicles [PS-*dendr*-$(NH_2)_8$] (*15*) through micellar rods [PS-*dendr*-$(NH_2)_{16}$, 12 nm in diameter], to spherical micelles [PS-*dendr*-$(NH_2)_{32}$, 10 to 20 nm in diameter] (Fig. 3).

The aggregation behavior observed is well described by the theory of Israelachvili *et al.* that relates amphiphile molecular shape and type of aggregation (*3*). Almost all of our aggregates, from spherical to inverted micelles, were formed by structures that differ only in the number of generations and hence in the size of the amphiphilic dendrimer head group. The measured diameters (10 to 20 nm) are the same order of magnitude as the estimated bilayers of the PS-dendrimer block copolymers. The stability of the aggregates formed is remarkable: Even spherical micelles could be made visible with the TEM techniques used (*16*). Dilution of the micellar cylinders did not yield a transition toward micelles, a phenomenon well known for traditional amphiphiles (*2*). Moreover, the results of the conductivity experiments are in agreement with the observed aggregation behavior. The lower generations exhibit reversed micellar properties in toluene, and their amphiphilic behavior is predominantly determined by the apolar PS chain. The cylindrical micelles of PS-*dendr*-$(NH_2)_{16}$ make it possible to stabilize both toluene and water as continuous phase, and therefore, a phase inversion point is observed that is strongly shifted toward higher volume fractions of toluene.

The aggregation phenomena described for our series of amphiphilic block copolymers with a polar head group that is confined in space show that, as the size of the head group increases, the polymers follow the theory of Israelachvili *et al.* qualitatively. The highly hydrophilic poly(propylene imine) dendrimer can be used as an amphiphile head group, thereby offering the opportunity to study a series of amphiphiles for which the chemical nature of the head group is unchanged and only the size and hence the shape is altered.

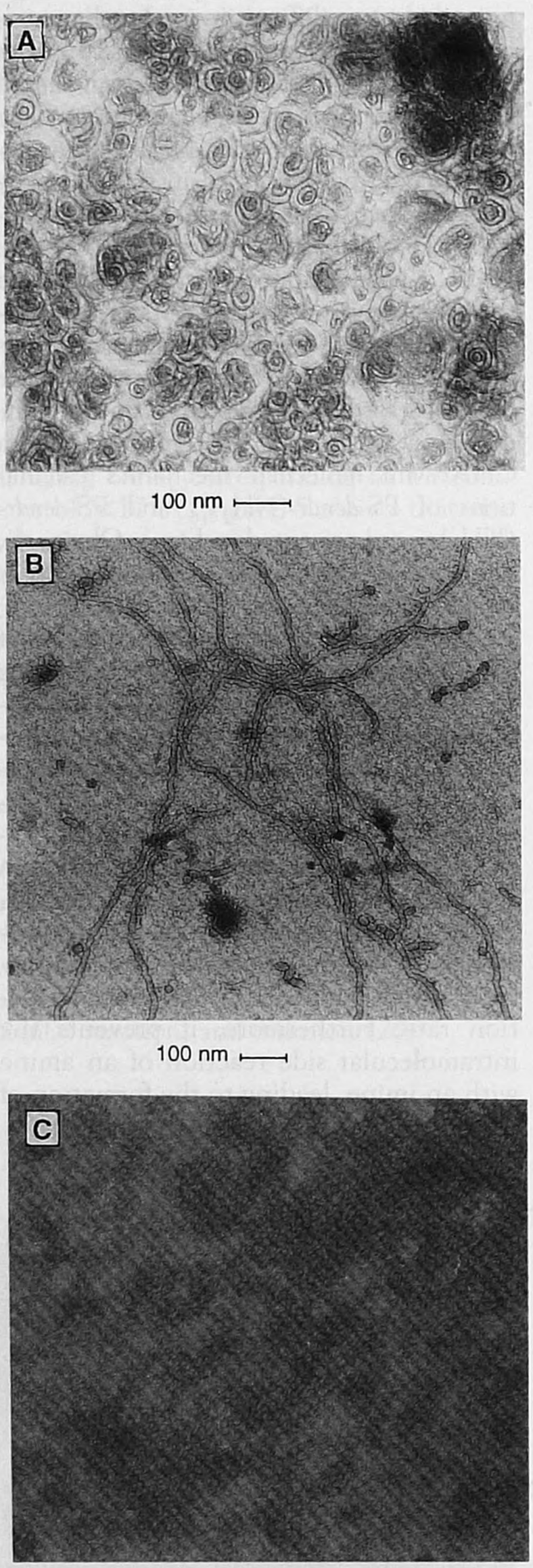

Fig. 3. TEM images of the aggregates. Aggregates of (**A**) PS-*dendr*-$(NH_2)_8$ (negative staining, ×107,000) exhibit vesicular structures. Aggregates of (**B**) PS-*dendr*-$(NH_2)_{16}$ (negative staining, ×84,000) take the form of micellar rods. Aggregates of (**C**) PS-*dendr*-$(NH_2)_{32}$ (negative staining, ×135,000) appear as spherical micelles.

REFERENCES AND NOTES

1. F. M. Menger and C. A. Littau, *J. Am. Chem. Soc.* **115**, 10083 (1993).
2. E. H. Lucassen-Reynders, *Anionic Surfactants, Physical Chemistry of Surfactant Action* (Surfactant Series, vol. 11, Dekker, New York, 1981); J. H. Fendler, *Membrane Mimetic Chemistry: Characterizations and Applications of Micelles, Microemulsions, Monolayers, Bilayers, Vesicles, Host Guest Systems, and Polyions* (Wiley-Interscience, Chichester, UK, 1982); S. A. Buckingham, C. J. Garvey, G. G. Warr, *J. Phys. Chem.* **97**, 10236 (1993).
3. J. N. Israelachvili, D. J. Mitchell, B. W. Ninham, *J. Chem. Soc. Faraday Trans. 2* **72**, 1525 (1976).
4. G. Riess, J. Nervo, D. Rogez, *Polym. Eng. Sci.* **8**, 634 (1977); Y. Gallot, J. Selb, P. Marie, A. Rameau, *Polym. Prepr. Am. Chem. Soc. Div. Polym. Chem.* **23**, 16 (1982); A. Desjardins and A. Eisenberg, *Macromolecules* **24**, 5779 (1991); R. Xu, M. A. Winnik, G. Riess, B. Chu, M. D. Croucher, *ibid.* **25**, 644 (1992); J. M. Denton, D. C. Duecker, E. D. Sprague, *J. Phys. Chem.* **97**, 756 (1993); V. Toncheva, R. Velichkova, G. Trossaert, E. J. Goethals, *Polym. Int.* **31**, 335 (1993).
5. D. A. Tomalia, A. M. Naylor, W. A. Goddard III, *Angew. Chem.* **102**, 119 (1990); J. M. J. Fréchet, *Science* **263**, 1710 (1994).
6. D. A. Tomalia, *Adv. Mater.* **6**, 529 (1994).
7. G. R. Newkome, A. Nayak, R. K. Behera, C. N. Moorefield, G. R. Baker, *J. Org. Chem.* **57**, 358 (1992); C. J. Hawker, K. L. Wooley, J. M. J. Fréchet, *J. Chem. Soc. Perkin Trans. 1* **1993**, 1287 (1993); V. Percec, P. Chu, M. Kawasumi, *Macromolecules* **27**, 4441 (1994); S. Watanabe and S. L. Regen, *J. Am. Chem. Soc.* **116**, 8855 (1994).
8. G. R. Newkome, C. N. Moorefield, J. Keith, G. R. Baker, G. Escamillo, *Angew. Chem.* **106**, 701 (1994); I. Gitsov, K. L. Wooley, J. M. J. Fréchet, *ibid.* **104**, 1282 (1992); I. Gitsov, K. L. Wooley, C. J. Hawker, P. Ivanova, J. M. J. Fréchet, *Macromolecules* **26**, 5621 (1993); I. Gitsov and J. M. J. Fréchet, *ibid.*, p. 6536.
9. T. M. Chapman, G. L. Hillyer, E. J. Mahan, K. A. Shaffer, *J. Am. Chem. Soc.* **116**, 11195 (1994).
10. X. F. Zhong and A. Eisenberg, *Macromolecules* **27**, 1751 (1994); *ibid.*, p. 4914.
11. E. M. M. de Brabander-van den Berg and E. W. Meijer, *Angew. Chem.* **105**, 1370 (1993).
12. Characterization of PS-*dendr*-$(CN)_n$ (n = 2, 4, 8,

16, or 32) and PS-*dendr*-$(NH_2)_n$ (n = 2, 4, 8, 16, or 32) was performed with ^{1}H NMR, ^{13}C NMR, and infrared spectroscopy. For example, PS-*dendr*-$(CN)_{32}$: ^{1}H NMR ($CDCl_3$) chemical shift δ 0.54 to 0.78 [br, 6H, $C\underline{H}_3$-CH_2-CH($C\underline{H}_3$)-(CH_2-CHPh)$_n$ (Ph, phenyl)], 0.78 to 2.74 (CH_3-$C\underline{H}_2$-$C\underline{H}(CH_3)$-($C\underline{H}_2$-$C\underline{H}$Ph)$_n$-CH_2-O-CH_2-CH_2-CH_2-N), 1.52 to 1.68 (br, 60H, N-CH_2-$C\underline{H}_2$-CH_2-N), 2.30 to 2.62 (br, 122H, O-CH_2-CH_2-$C\underline{H}_2$-N + N-CH_2-CH_2-$C\underline{H}_2$-N), 2.45 (t, J = 6.6 Hz, 64H, N-CH_2-$C\underline{H}_2$-CN), 2.82 (t, J = 6.6 Hz, 64H, N-$C\underline{H}_2$-CH_2-CN), 3.13 to 3.45 (br, 4H, CH_2-CHPh-$C\underline{H}_2$-O-$C\underline{H}_2$-CH_2-CH_2-N), 6.25 to 7.32 [(CH_2-$C\underline{H}$Ph)$_n$]; ^{13}C NMR ($CDCl_3$) δ 11.0 to 11.4 [br, $\underline{C}H_3$-CH_2-CH(CH_3)-(CH_2-CHPh)$_n$], 16.8 (32x, N-CH_2-$\underline{C}H_2$-CN), 18.8 to 20.0 [br, CH_3-CH_2-CH($\underline{C}H_3$)-(CH_2-CHPh)$_n$], 23.7 (2C+4C+8C, N-CH_2-$\underline{C}H_2$-CH_2-N), 24.6 (16C, N-CH_2-$\underline{C}H_2$-CH_2-N), 26.5 (1C, O-CH_2-$\underline{C}H_2$-CH_2-N), 28.1 to 30.2 [br, CH_3-$\underline{C}H_2$-CH(CH_3)-(CH_2-CHPh)$_n$], 31.3 [CH_3-CH_2-$\underline{C}H$-(CH_3)-(CH_2-CHPh)$_n$], 40.1 [CH_3-CH_2-CH(CH_3)-(CH_2-$\underline{C}H$Ph)$_n$], 39.8 to 46.6 [br, CH_3-CH_2-CH(CH_3)-($\underline{C}H_2$-CHPh)$_n$], 49.0 (32C, N-$\underline{C}H_2$-CH_2-CN), 52.0 to 50.4 (br, 1C, O-CH_2-CH_2-$\underline{C}H_2$-N, 2C+2C+4C+4C+8C+8C+16C+16C, N-$\underline{C}H_2$-CH_2-$\underline{C}H_2$-N), 69.6 to 69.2 [br, (CH_2-CHPh)$_n$-CH_2-O-$\underline{C}H_2$-CH_2-CH_2-N], 75.2 to 76.2 [br, (CH_2-CHPh)$_n$-$\underline{C}H_2$-O-CH_2-CH_2-CH_2-N], 118.7 (32C, $\underline{C}$N), 125.2 to 127.0 (br, CH_2-CH$\underline{Ph}_{para}$), 127.1 to 130.0 (br, CH_2-CH$\underline{Ph}_{ortho+meta}$), 145.1 to 146.6 (br, CH_2-CH$\underline{Ph}_{ipso}$); IR: frequency $\nu_{C\equiv N}$, 2246 cm^{-1}.

13. The dendrimer part is confined in space, but a variety of PS chain conformations is possible; we show an extended chain, similar to the representations of traditional surfactants.
14. The aqueous aggregates were prepared according to the following procedure: the amphiphiles were dissolved in 2 ml of toluene or tetrahydrofuran. After the addition of 25 ml of water, the organic solvents were evaporated and stable aggregates were formed. The PS-*dendr*-$(NH_2)_{32}$ system even gave a clear solution in water, thereby indicating a remarkably low Krafft temperature for this structure.
15. The observed vesicular structures show a resemblance to the structure proposed by Kunitake *et al.* [T. Kunitake, N. Kimizuka, N. Higashi, N. Nakashima, *J. Am. Chem. Soc.* **106**, 1978 (1984); T. Kunitake, M. Nagai, H. Yanagi, K. Takarabe, N. Nakashima, *J. Macromol. Sci. Chem.* **21** (no. 8–9), 1237 (1984)].
16. For the techniques used to observe spherical micelles with TEM, see O. Regev, C. Kang, A. Khan, *J. Phys. Chem.* **98**, 6619 (1994).
17. We thank E. M. M. de Brabander-van den Berg for discussions on dendrimer synthesis; J. Joosten and A. Moussaid for performing the DLS measurements; H. van Nunen, H. Geurts, and Y. Engelen for assistance with the TEM measurements; and A. van Kraay for the molecular modeling. This research was supported under a DSM Research unrestricted research grant.

4 January 1995; accepted 28 March 1995

EUVE Observations of Jupiter During the Impact of Comet Shoemaker-Levy 9

G. Randall Gladstone, Doyle T. Hall, J. Hunter Waite Jr.

The Extreme Ultraviolet Explorer (EUVE) satellite conducted extensive observations of the jovian system before, during, and after the impact of the fragments of comet Shoemaker-Levy 9 in July 1994. About 2 to 4 hours after the impacts of several of the larger fragments, the brightness of the neutral helium (He I) resonance line at 58.4 nanometers temporarily increased by a factor of about 10. The transient 58.4-nanometer brightenings are most simply explained by resonant scattering of sunlight from the widespread high-altitude remnants of the larger impact plumes. Other possible sources of emission, such as electron impact excitation of He or radiative recombination of He^+, may contribute to the observed signal.

Observations of extreme ultraviolet (EUV) emissions from the neutral helium resonance line at 58.4 nm were recognized years ago as an excellent means for studying the upper atmosphere of Jupiter (*1*). The He I 58.4-nm line on Jupiter is principally excited by resonant scattering of sunlight (*2*), and its brightness depends primarily on the relative abundances of helium and hydrogen in the jovian upper atmosphere. Both molecular and atomic hydrogen are strong absorbers of 58.4-nm radiation; because they are both lighter than helium, their relative abundances increase in the region above the well-mixed part of the atmosphere, and the probability of absorption for a 58.4-nm photon increases likewise. The altitude separating the well-mixed lower region of the atmosphere (where all long-lived species share a common altitude dependence or scale height) from the diffusive-equilibrium upper atmosphere (where each long-lived species has a different scale height, according to mass) is known as the homopause. The homopause level depends on upper atmosphere dynamics. With vigorous circulation, the homopause will be at high altitude; with more sluggish circulation, it will drop to a lower altitude. Through absorption by the overlying column of H and H_2, the brightness of the He I 58.4-nm emission on Jupiter provides a direct indication of the altitude of the homopause and thus provides information about the dynamics of the jovian upper atmosphere. The strength of the solar He I 58.4-nm line (*3*) and the chemical inactivity of helium (*4*) make the 58.4-nm brightness an ideal diagnostic of vertical mixing in the upper atmospheres of the giant planets.

The Pioneer 10 EUV photometer measured a 5.1-rayleigh (R) (*5*) signal in late 1973 that was attributed to the He I 58.4-nm feature (*6*), although in retrospect, the observation may have been contaminated by EUV emissions from sulfur and oxygen ions in the then unknown Io plasma torus. The ultraviolet spectrometer (UVS) experiments on Voyager 1 and 2 measured He I 58.4-nm brightnesses of 5.2 and 4.4 R, respectively, averaged over much of the dayside disk, during the 1979 encounters (*7*). The brightness differences between the two Voyager UVS measurements are most probably caused by solar cycle variations in the solar He I 58.4-nm line (*3*).

After the Voyager flybys, there were no further observations of EUV emissions from Jupiter until the launch of EUVE in June 1992 (*8*). The EUVE observations are made with three spectrographs that cover a wavelength band from 7.0 to 76.0 nm with a resolving power ($\lambda/\Delta\lambda$) of about 200 to 400 for point sources. The spectrographs share the same grazing-incidence mirror, have circular fields of view about 2° in diameter, and are capable of imaging monochromatic emissions (*9*). For moving sources (such as planets), the photons may be remapped into a target-centered frame of reference by using the arrival times and appropriate ephemerides for the spacecraft and the target (*10*).

Observations of the Jupiter system were made by EUVE in April 1993, and a rich spectrum of the Io plasma torus was obtained. However, no excess He I at 58.4 nm that could have been associated with Jupiter was found (*11*). Observing jovian He I emitting at 58.4 nm is difficult from EUVE's 520-km altitude because of the resonant scattering of sunlight by Earth's extended helium atmosphere or geocorona. The He I 58.4-nm geocoronal foreground emissions are mildly optically thick and depend primarily on solar zenith angle, but they vary rather slowly with look direction at the altitude of EUVE (*12*). The darkest part of the sky to look toward is antisunward at orbital midnight. During EUVE's all-sky survey, this part of the sky was examined routinely for 6 months, from July 1992 until January 1993. A study of the geocoronal brightness in the antisolar direction from 25 July to 19 August 1992 yielded an average brightness of 1.3 R (*13*). In other directions, the 58.4-nm airglow is usually larger. In particular, observations made from within the Earth's shadow at 90° to the Earth-sun line (approximately the geometry during the week of the comet impacts) generally show helium geocoronal airglow brightnesses about twice those in the antisunward direction. The geocoronal He I 58.4-nm brightness was 2.2 R during the April 1993 observations, and the corre-

G. R. Gladstone and J. H. Waite Jr., Department of Space Sciences, Southwest Research Institute, 6220 Culebra Road, San Antonio, TX 78228, USA.
D. T. Hall, Center for Astrophysical Sciences, Department of Physics and Astronomy, Johns Hopkins University, Baltimore, MD 21218, USA.